OPEN

The strange flight behaviour of slowly spinning soccer balls

Taketo Mizota[1], Kouhei Kurogi[1]*, Yuji Ohya[2], Atsushi Okajima[3], Takeshi Naruo[4] & Yoshiyuki Kawamura[1]

[1]Department of Intelligent Mechanical Engineering, Fukuoka Institute of Technology, 3-30-1, Wajiro-higashi, Higashi-ku, Fukuoka, 811-0295, Japan, [2]Director of Research Institute for Applied Mechanics, Kyushu University, 6-1, Kasuga-koen, Kasuga-shi, Fukuoka, 816-8580, Japan, [3]Professor Emeritus of Kanazawa University, 4-7-11, Suzumidai, Kanazawa, 920-1161, Japan, [4]MIZUNO Co., 1-12-35, Nanko-kita, Suminoe-ku, Osaka, 559-8510, Japan.

The strange three-dimensional flight behaviour of slowly spinning soccer balls is one of the most interesting and unknown phenomenon associated with the trajectories of sports balls. Many spectators have experienced numerous exciting and emotional instances while observing the curious flight behaviour of these balls. We examine the aerodynamic mechanisms of erratic ball behaviours through real flight observations, unsteady force measurements and flow pattern visualisations. The strange behaviour is elucidated by the relationship between the unsteady forces on the ball and the wake flow. The irregular changes in position for twin longitudinal vortices have already been discovered in the supercritical Reynolds number region of a sphere with a smooth surface. This finding is applicable to the strange behaviour of the flight of soccer balls with this supercritical flow. The players, spectators, and television viewers will gain greater insight into the effects of soccer ball flights.

No reasonable qualitative aerodynamic explanation exists for the mechanism of the erratic flight trajectory of soccer balls. In the subcritical Reynolds (Re) number region, vortex shedding from spheres with smooth surfaces was previously investigated[1]. For higher Re numbers, some observations of steady fluid forces on spheres with smooth surfaces were reported[2], including the effect of surface roughness[3] on the drag crisis phenomenon. The mechanism of unsteady forces acting on smooth spheres with supercritical Re numbers was explained by Taneda[4] through observing bound and wake vortices, i.e., the twin longitudinal vortices irregularly move on the surface of a sphere and in a wake. A model calculation of ring vortex shedding was performed to explain the generations of unsteady lift and drag forces on spheres[5]. Some research[6] has also indicated that the cause of the erratic behaviour of slowly spinning soccer balls is strongly related to the findings of Taneda. The steady aerodynamic forces were calculated by using the methods of computational fluid dynamics, and the flight trajectory estimation was conducted under the quasi-steady-state approximation with the ball slow rotation[7]. The aerodynamic forces of strange soccer ball flight trajectories depend on the Re number and spin parameter (Sp), where Sp is a non-dimensional parameter of (ball surface speed due to spin)/(ball speed).

Results

Strange trajectory of ball flight observations. The initial speed of a slowly spinning ball that was kicked by a soccer player, Keisuke Honda[8] was 104 km/h (28.9 m/s), and a goalkeeper cannot immediately predict the flight trajectory of a soccer ball because of the violent erratic behaviour, so he can hardly move to defend the ball. A stroboscopic image from a free-fall experiment under natural low-wind conditions is shown in Figure 1a. A strange displacement of the soccer ball was observed during free-fall. The maximum amplitude within the horizontal plane (Y-Z plane) was approximately 0.75 m during a 4.3 s period, the ball shift frequency was approximately f = 1.2 Hz, and, the maximum speed was approximately 22.5 m/s in Figure 2a. In this scenario, the ball continued to accelerate. According to the measured drag coefficient value, the final speed of the ball was estimated to be approximately 30 m/s under a higher free-fall drop test. The relationships between the lift and side forces are indicated in Figure 1b. In this free-fall experiment, the lift and side force directions were defined toward the upward and right directions, respectively, in Figure 1a. This abrupt change in aerodynamic coefficients (C_L, C_S) is a characteristic feature of the final falling stage due to faster ball speeds.

The flight trajectory results obtained using a shooting machine also demonstrated strange erratic behaviour, as shown in Figures 1c, d, and e (U = 82 km/h, 22.8 m/s) and Figures 1f, g and h (105 km/h, 29.2 m/s), including the Y-Z plane trajectory (Figures 1d and g) and side force coefficient (Cs) time traces (Figures 1e and h). We observed erratic trajectories along dissimilar flights with probabilities greater than 80%. The ball shift magnitudes
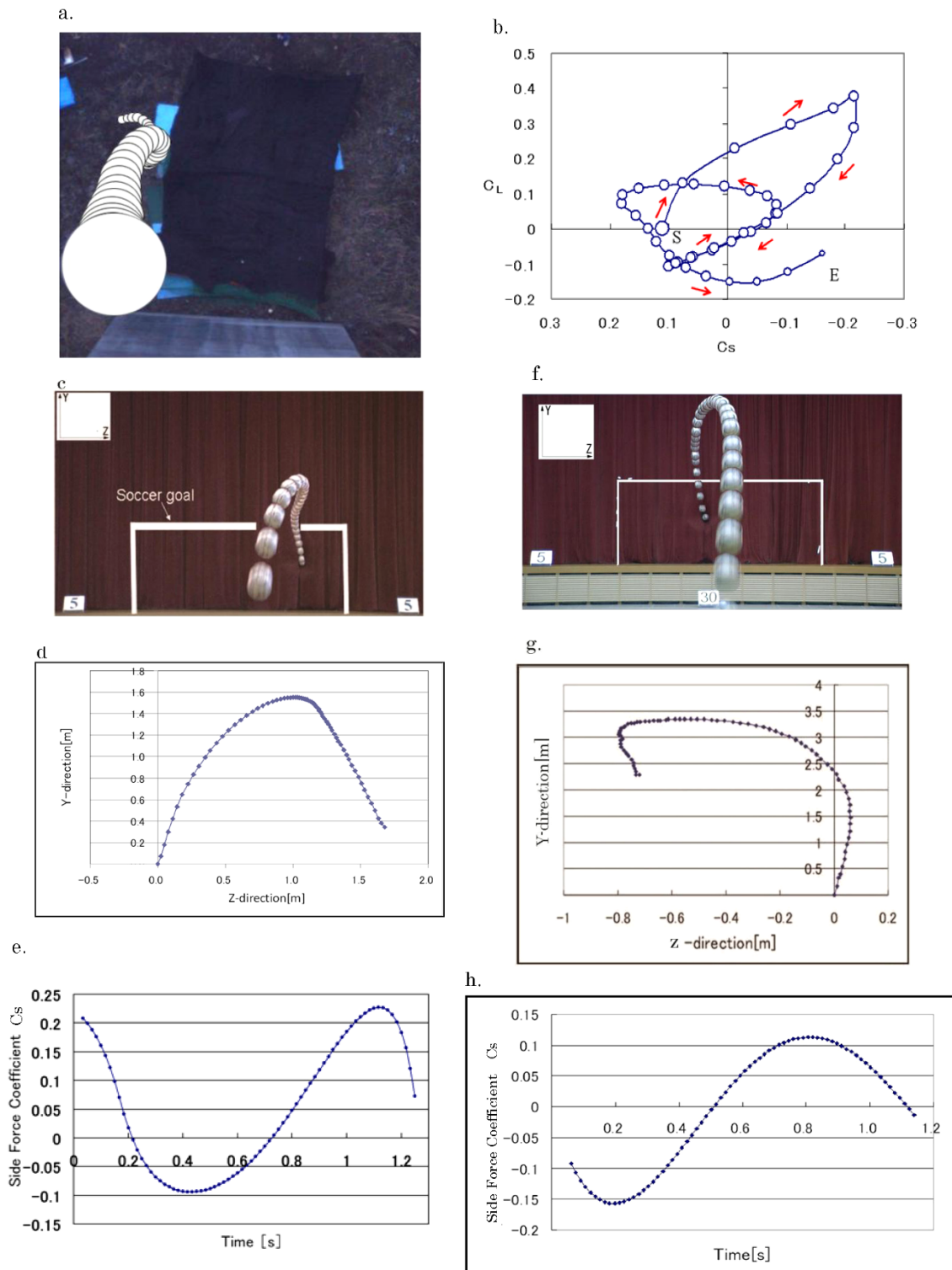
Figure 1 | Free-fall and free-flight ball trajectories of soccer balls and aerodynamic side force coefficients. (a), A stroboscopic image of a 65 m free-fall experiment. The ball had a 250 fps high-speed camera located on a bridge plate facing the ground. The spin rate (N) was less than 1/16 rps, and the spin parameter (Sp) was 0.002. Here, the Sp was defined as $Sp = \pi Nd/U$. (b), The aerodynamic force coefficients (C_L and C_S) were calculated from the position image every second with a two-step time differentiation. The red arrows denote the time sequences from S: (observations start) to E; (final stage). C_D, C_L, and C_S represent the aerodynamic force coefficients of the drag, lift, and side forces, respectively, at time t. $(C_D, C_L, C_S) = (D, L, S)/0.5\rho\ U^2A$. The directions include +drag (D, gravity force direction), +lift (L, upward in this figure and +side force (S, direction to the right). ρ represents air density, U represents the ball speed, and, A represents the ball area with diameter (d) = $\pi d^2/4$. The origin of this diagram does not correspond to (a). (c–e), (f–h), Two examples of a three-dimensional flight using a shooting machine. (c) and (f) display stroboscopic images of balls launched by the machine; the initial speeds in (c) and (f) were U_0 = 82 km/s (22.8 m/s) and 105 km/h (29.2 m/s), respectively. The spin rates were approximately 1 rps, and the Sp was = 0.03. (d) and (g) present displacements in the Y-Z plane based on the stroboscopic image in (c) and (f). (e), (h), Time traces of the side force coefficient (C_S). The C_S amplitude and period were 0.10–0.15 and 1.3 s, respectively, in both cases. The accuracy of the measured ball position may be within +5.0 to −5.0 cm, due to the digitised pixel number.
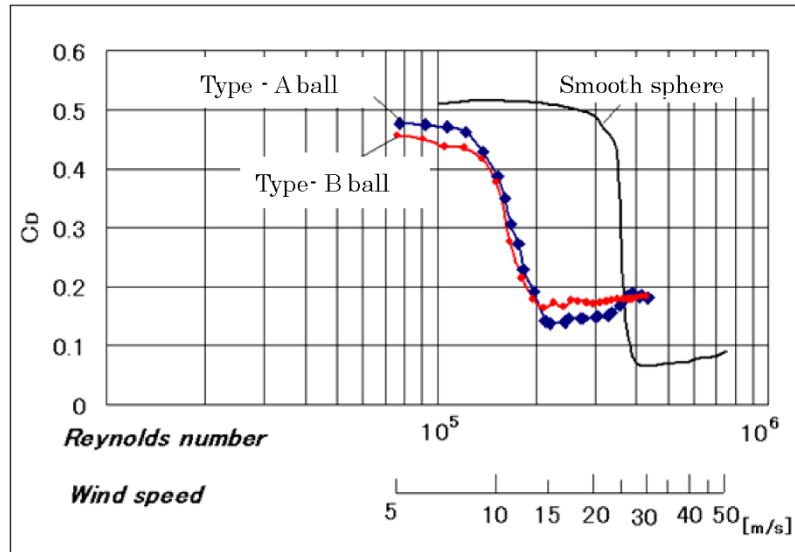
Figure 2 | **Time-averaged drag coefficients of a sphere with a smooth surface and soccer balls at varied Re numbers.** (a), The drag coefficients (C_D) of soccer balls and spheres with smooth surfaces. The drag coefficients depend on $Re = Ud/\nu$, where, U is the wind tunnel air speed, (U = 5–30 m/s), d is the ball diameter, (d = 0.225 m), and ν is the dynamic viscosity of the air. The drag crisis appeared at approximately U = 25 m/s for a smooth sphere and 10 m/s for the soccer balls. (b), Type-A ball, +Teamgeist, Molten, the groove depth was 1.51 mm (average value of 10 locations on a random sample), and the standard deviation was 0.042 mm. (c), Type-B ball, truncated icosahedron, Mizuno: the groove depth was 1.69 mm (average value of 10 locations on a random sample), and the standard deviation was 0.058 mm. The representation of the ball photographs in (b) and (c) are under the permissions of Adidas Co. and MIZUNO Co.

in the Y-Z plane perpendicular to the beam of the camera image were calculated. The results did not indicate a smooth shift of aerodynamic forces in the Y and Z directions. In Figure 1g, the initial direction of the ball is +Z, the side forces are acting toward −Z (Figure 1h), and the maximum displacement is approximately 0.9 m. As a result, the amplitude of the side force coefficient (C_S) and the period are within the approximate range of 0.1–0.15 and 1.3 s, respectively, as shown in Figures 1e and h. The Sp values were 0.002 in the free-fall experiment and approximately 0.03 in the machine shooting experiments, respectively.

Time-averaged drag on soccer balls and spheres with smooth surfaces. The time-averaged drag (C_D) on the soccer balls was measured in a wind tunnel with uniform flow, as indicated in Figure 2a with smooth-surfaced spheres[9]. For a sphere with a smooth surface, the phenomenon of drag crisis appears at $Re = 3.5 \times 10^5$, under a low-turbulence flow. This result is due to the natural transition from the laminar boundary layer to the turbulent boundary layer. However, many patches exist on surface of a soccer ball, which are surrounded

by regions with approximate depths of 1.50–1.60 mm, and artificially promote the boundary layer flow transition from a laminar flow to turbulent flow, resulting in the drag crisis in the lower Re number region. These surface roughness effects of the soccer balls correspond well with spheres[3] and soccer balls[10]. The supercritical Re number flow around soccer balls is similar to the flow around smooth spheres ($Re = 3.8 \times 10^5$ (U = 26.0 m/s, in soccer ball diameter)), which is higher than $Re = 2.0 \times 10^5$ (U = 13.2 m/s) as shown in Figures 2b and c for Type-A and Type-B balls, respectively. Experiments of the unsteady force measurements and flow visualisations are conducted using a Type-A ball in this study.

Unsteady aerodynamic forces and flight trajectory. The unsteady aerodynamic forces on a Type-A ball (Figure 2b) were measured with a soccer ball at rest in a wind tunnel flow. The coefficients of unsteady lift (C_L) and side force (C_S) for U = 22 m/s are shown in Figure 3a. These measured results exhibit purely random characteristics, even when assessed by spectrum analyses. In this example, the results were simultaneously constant for a few seconds as they centred for
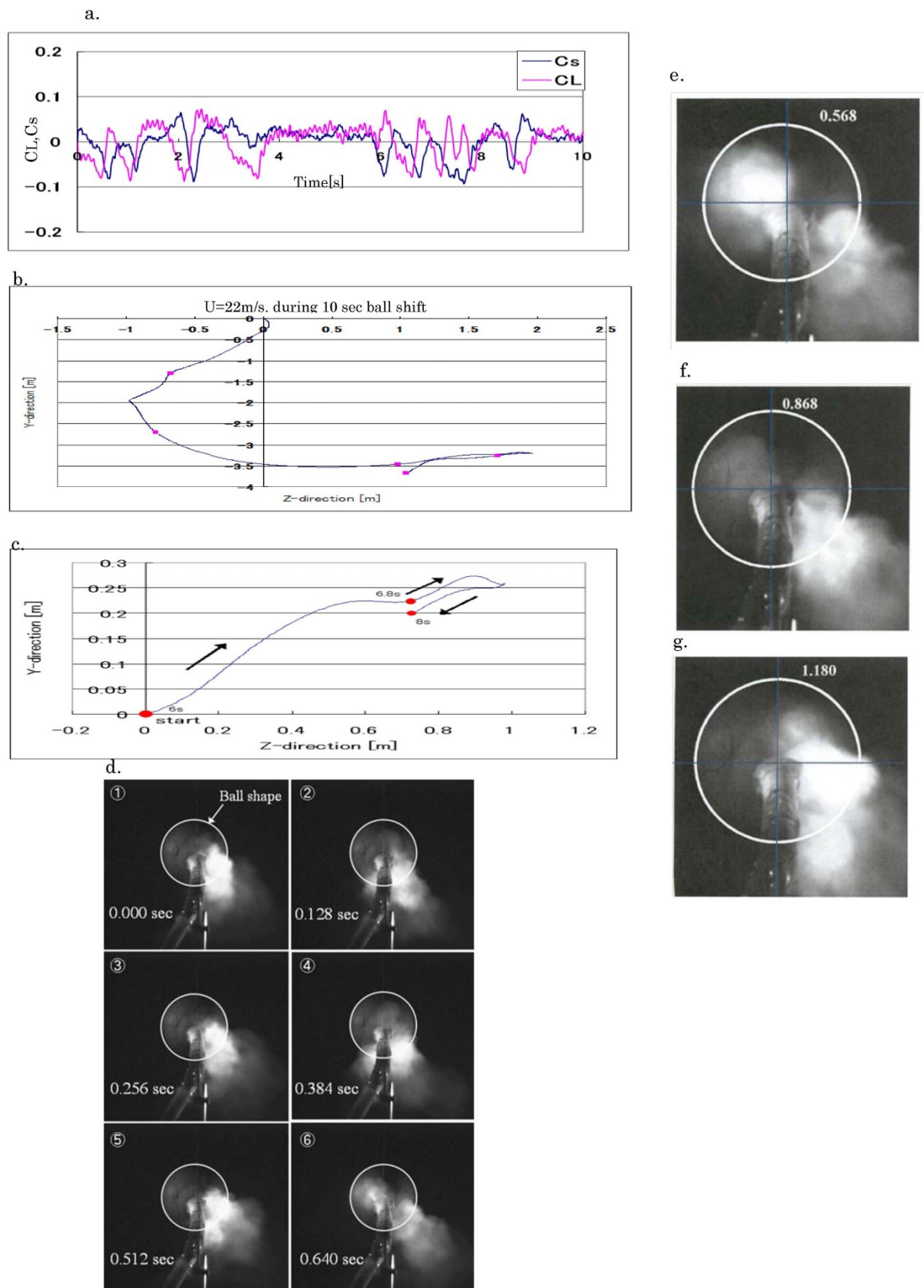
Figure 3 | Unsteady forces on soccer balls, ball shift magnitudes, and flow patterns visualised using the smoke method. (a), Unsteady aerodynamic forces (C_L, red line) and (Cs, blue line) on the type-A ball during a 10 s period ($Re = 3.3 \times 10^5$, $U = 22.0$ m/s, 50 Hz sampling frequency). (b), Ten second ball shift in the Y-Z plane ($U = 22.0$ m/s). (c), Magnification of the Y-Z plane ball shift between 6 and 8 s ($U = 22.0$ m/s). (d), Images for each 0.128 s time step. During these periods, the vortices primarily existed in the lower right position with small variations. The two longitudinal vortices were in close proximity. Between 0.512 and 0.640 s, one vortex separated as it passed two vortices. (e–g), The mode change in the twin vortex images (e) to one vortex (f), followed by the two vortices or twin vortex pattern (g).
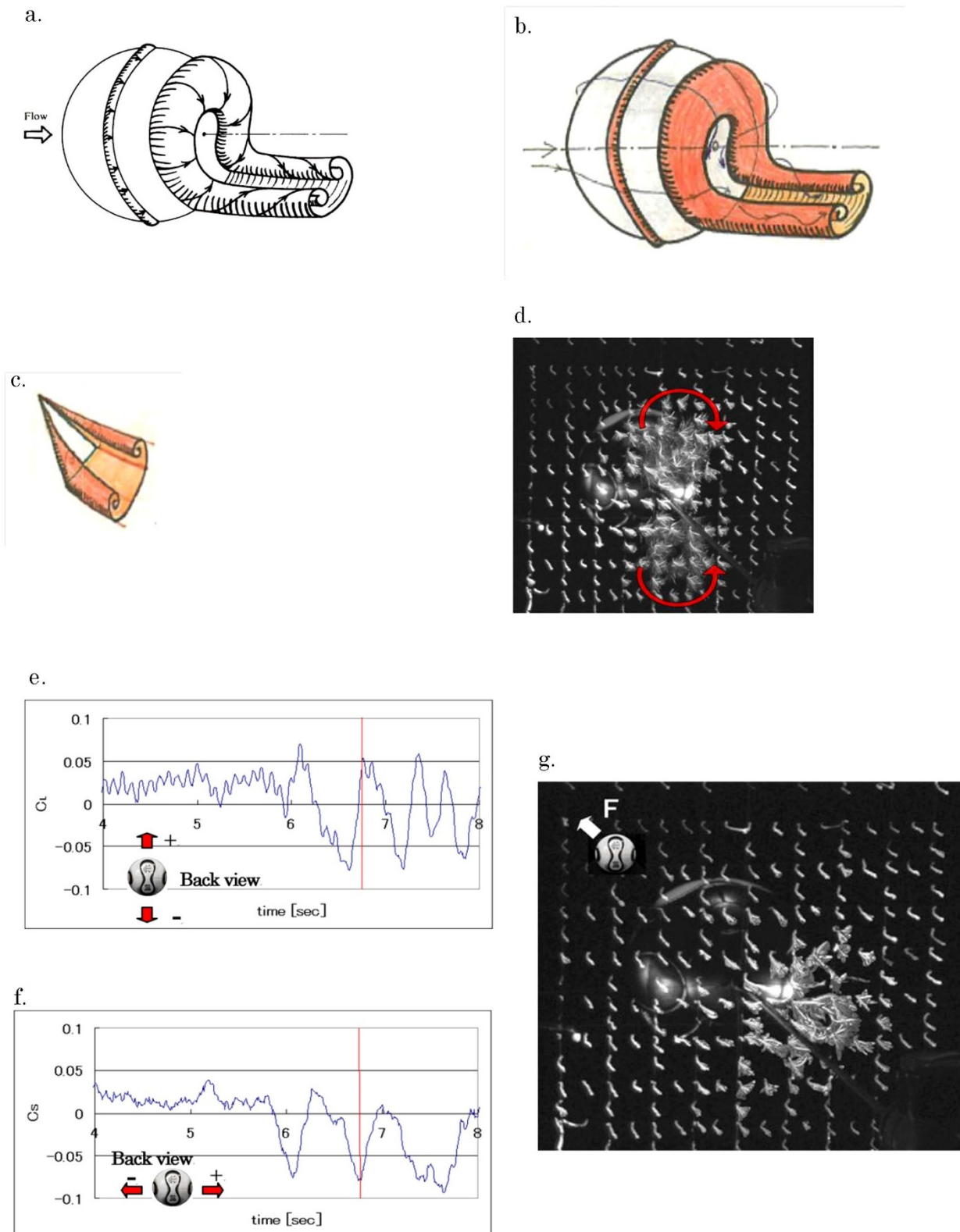
Figure 4 | Ω-shaped and two longitudinal vortices of a smooth sphere by Taneda[4] and the relationships between the unsteady forces and flow around a soccer ball. (a), An image obtained by Taneda[4] of the flow around a smooth sphere at the supercritical Re number, Re = 3.8 × 10⁵. This flow is an integrated streak line of the surface boundary layer into a Ω-shaped or U-type vortex and two-line flows of the longitudinal vortices. (b), The colour image was reproduced from the research notebook of Dr. Taneda with permission from his bereaved family. This figure was dated March 9, 1976. (c), The flow around the delta wing in his sketch. This figure was dated February 24, 1976. (d), Typical twin longitudinal vortices as shown in a. U = 26.0 m/s with 25 integrated frames during a 0.1 s period. (e–f), Unsteady aerodynamic force coefficients (C_L and Cs) at 4–8 s, in Figure 3a. (g), The flow pattern observed in multiple images in 25 frames during the 0.1 s period of 6.75–6.85 s centred around the red lines of e and f. A longitudinal vortex exists in the lower-right directions. The resultant aerodynamic force (F), which is indicated by the arrow in (g), was oriented in the opposite direction of the vortex position at the symmetrical position of the ball centre axes.

approximately 5 s. The ball shift magnitudes were obtained by a two-step time integration procedure, as shown in Figure 3b (10 s) and Figure 3c (2 s during a period of approximately 6.0–8.0 s). In these calculations, the ball speeds are constant at 22.0 m/s and the gravity force is neglected to emphasise the effect of aerodynamic forces. For 1.2 s during an approximately 6.8–8.0 s period, the ball shifts 0.3 m toward the right and rapidly returns to the reverse direction by 0.3 m.

These unsteady aerodynamic forces are induced by unsteady flow in the wake of the ball. High-speed camera images of condensed smoke in the longitudinal vortex flows, which are mentioned in the Discussion section below, are shown in Figures 3d①–⑥ and Figures 3e–g. The frame rate of the high-speed camera was 250 fps, with images taken every 0.004 s, and the images in these figures represent every 0.128 s. During these sampling times, the dominant positions of the vortex fall in the lower-right position. Through precise observations within this sequence of 0.640 s, we were able to recognise that the phases of these vortices change every 0.128 s. The pattern of vortex phase undergoes various changes from a pair of adjacent twin vortices to a pair of clearly separated twin vortices (Figure 3d 0.384 s → Figure 3d 0.512 s or 0.640 s) and from a pair of clearly separated twin vortices to a pair of adjacent twin vortices (Figure 3e → Figures 3f and g) within a short time period. Other examples illustrate either a pair of clearly separated twin vortices during a 0.34 s period or no phase change for more than 1 s.

Discussion

Instantaneous flow images of smooth spheres[4] in the supercritical Re flow region are illustrated in Figure 4a, where the three-dimensional boundary layer flow on the surface is integrated into a Ω-shaped vortex that transforms into twin longitudinal vortices. Figure 4b displays the flow image in the same region, which appeared in the article by Taneda[4]; the colour image was directly copied from his research notebook, provided by his bereaved family. This conceptual sketch, which appears very similar to the bound and tip vortices produced by airplane wings, as well as to the general flow around three-dimensional bodies, is a reasonable shape from a topological standpoint, as is his sketch of the flow around a delta wing in Figure 4c. However, the asymmetric vortices of the sphere have the freedom to rotate or oscillate around a central axis in the main flow direction behind a sphere. The reaction force to a momentum change by the unsteady vortex flow is the main cause of the unsteady aerodynamic force on a sphere.

The other observation of flow behind the soccer ball, which is shown in Figure 4d, yields U = 26.0 m/s, 250 fps and an integration of 25 frames during a 0.1 s period. The integrated tuft images indicate clear twin vortices and illustrate the longitudinal twin vortex flow.

Simultaneous observations of the flow visualisations and unsteady force measurements are shown in Figures 4e and f, (the same series as that shown in Figures 3a). In the first 2 s, both amplitudes were small; then, the amplitude suddenly began to oscillate. The unsteady lift force (C_L) and side force (Cs) amplitudes were approximately 0.05, and the frequency was not constant, ranging from 0.7 to 2.5 Hz. In both figures, the vertical red lines indicate t = 6.80 s. Flow visualisation via the tuft method, with an integration of 25 frames during 6.75–6.85 s, is shown in Figure 4g. The resultant force vector **F** of the unsteady lift and side forces is oriented toward the upper and left direction, as shown in Figure 4g. In this instance, the longitudinal vortex is observed to be toward the right and downward directions, which is opposite the direction of **F**.

In the relationship between the unsteady flow momentum and aerodynamic forces, a quasi-steady-state flow condition must be ensured as a precondition. The Strouhal number is an index of this condition, being the order 0.01 (St = f·d/U, where: f = 1.0 Hz, U = 20 m/s and d (ball diameter)) = 0.225 m). This small value indicates that the flow phenomenon may be treated as quasi-steady-state conditions.

The strange change in the flight trajectory of a slowly spinning soccer ball occurs for masses ranging from 0.410 to 0.450 kg. For example, the mass ratio value of m/(ρV) = 64 was suitable for the strange trajectory flight caused by unsteady aerodynamic forces. For the value of 64, m is the mass of the soccer ball (0.425 kg), ρ is the air densety (1.205 kg/m³) under 1 atm and 20°C, and V is to the volume of the soccer ball.

In the case of spinning balls, the unsteady resultant lift and side forces may disappear. An increase in the rotational speed of the ball generates the steady Magnus force, which should result in a curved ball. The ball rotational speeds values (N) s under various conditions, ranging from purely random conditions to nearly steady conditions, were determined experimentally to be approximately two to three rotations per second[11].

In contrast, in the free-fall experiments (Figure 1a), the ball rotated by less than 1/8th of a full rotation during the 65 m fall process, in which the Sp value was 0.002. In the machine shooting experiments (Figure c and f), the ball rotated less than one round over the 30 m trajectory, in which the value of Sp was approximately 0.03.

According to both observations of the free-fall (Sp = 0.002, N = 0.06 rps) and machine shooting (Sp = 0.03, N = 1 rps) experiments, there were no significant differences in the strange behaviour of the flight. The seams on a soccer ball play an essential role in the transition from laminar to turbulent flow. Although the seam patterns of the commercial soccer balls influence the static characteristics of C_D, such as the drag crisis, by the effects of the boundary layer transition, we did not observe a significant difference in the strange unsteady behaviour of the balls, with the different seam patterns used in this study.

The results of the free-fall, ball shooting, and wind tunnel experiments indicated that the seams on the soccer ball surface promoted the transition of boundary layer from laminar to turbulent flow and yielded the supercritical Re number flow, accompanied with the Ω vortex and the twin longitudinal vortices around soccer balls. Thus, the random behaviour of the slowly spinning soccer ball's flight is mainly caused by the unstable movements of these vortices.

Incidentally, strangely behaving volleyballs that undergo floater serves exhibit the same type of moving behaviour and aerodynamic as that of soccer balls. Although scientific viewpoints regarding similar types of sports ball phenomena have generally been ignored in the literature, this finding may evoke scientific interests in sports science.

Methods

Free-fall experiments. Free-fall experiments were conducted on the Aso-Choyo Big Bridge, which has 65 m-high floorboards, in Choyo Village, Kumamoto, Japan. The natural wind was calm, with wind speeds ranging from 0 to 0.4 m/s. All of the aerodynamic coefficients in Figure 1 were calculated using the experimental results of the ball speeds. The ball speeds were detected with the functional relationship between the digitised area of the ball and the flight distance from the sequential photographs of a high-speed camera. This relationship was clarified by a calibration test.

Soccer ball shooting experiments were conducted with a machine containing two rollers with 340 mm diameters, urethane surfaces, and 650 mm-long shafts. The balls were shot from between two rollers and controlled by uniformly varying the rotational speed.

From the unsteady aerodynamic forces (C_D, C_L, C_S : t), we can easily obtain the flight trajectory data of the balls (x, y, z: t) using a two-step time integration. The reverse process for the calculation of the aerodynamic forces was performed using two-step time differentiations.

Wind tunnel experiments. Some of the aerodynamic forces were measured in the Boundary Layer Wind Tunnel at the Research Institute for Applied Mechanics of Kyushu University. The test section was 3.6 m wide, 2.0 m high, and 15 m long. The wind velocities were U = 0–30 m/s with less than <0.5% turbulence.The three-components load cell exhibited favourable linearity and no interference. The natural frequency of this system was approximately 19 Hz and was sufficiently high to enable measuring the forces with a frequency of less than <5 Hz. The data sampling frequency of the unsteady forces was a 50 Hz. The wind forces on the

connection parts between a ball and load cell were detected to be approximately 3.1–9.6% of the total drag forces and were subtracted from the total drag forces. However, the lift and side forces were essentially negligible and small.

The soft tuft grid was located 0.1 m behind the rear surface of the ball and was 1.5 m wide and 1.8 m high. The mesh grid sizes were 50 × 50 and 25 × 25 mm and constructed with piano wires of 0.3 mm diameters. Firework smoke was generated in a pressurized box arranged beneath the wind tunnel floor. The smoke was introduced in the rear surface of the ball through a tube and, under negative pressure in the wind tunnel. The longitudinal vortex, which behaved similarly to that of the tuft and smoke, was captured by 250 fps frame rates with a high-speed camera.

1. Sakamoto, H. & Haniu, H. A study on vortex shedding from sphere in a uniform flow. *Trans. of the ASME* **112**, 386–392 (1990).
2. Achenbach, E. Experiments on the flow past spheres at very high Reynolds numbers. *J. Fluid Mech.* **54**, 565–575 (1972).
3. Achenbach, E. The effects of surface roughness and tunnel blockage on the flow past spheres. *J. Fluid Mech.* **65**, 113–125 (1975).
4. Taneda, S. Visual observations of the flow past a sphere at Reynolds numbers between 10^4 and 10^6. *J. Fluid Mech.* **85**, 187–192 (1978).
5. Home, M. S., Lauchle, G. C. & Wang, J. Aerodynamic lift and drag fluctuations of a sphere. *J. Fluid Mech.* **436**, 2001, 41–57 (2001).
6. Mizota, T. *et al.* The measurement of unsteady aerodynamic force acting on a low turn soccer ball by a wind tunnel experiment. *Proc. JSME, Fluid Engineering Conference*, **07–16**, 208–211 (2007).
7. Barber, S., Chin, S. B. & Carre, M. J. Sports ball aerodynamics: a numerical study of the erratic motion of soccer balls. *Computational Fluid Dynamics*, **38**, 1091–1100 (2009).
8. God techniques by Honda, K., May 16, 2007 Hong Kong, U-22 Hong Kong vs. U-22 Japan, Beijing Olympic Asia-2nd preliminary match, (2007). http://www.youtube.com/watch?v=MdrXnsUkzDw: in Japanese, accessed in March 2013.
9. Schlichting, H. *Boundary-Layer Theory.* Pergamon Press, London, p. 17 (1979).
10. Asai, T. *et al.* Basic research of soccer ball aerodynamic. *JSME, Fluid dynamics division*, **05–32**, 236 (2005).
11. Lingbo, Z. *et al.* Non-spinning and spinning soccer ball aerodynamics with wind tunnel and shooting experiments. *Proc. 9th Conference of the International Sports Engineering Association (ISEA),* July 7–13, Lowell Mas., http://continuinged.uml.edu/isea2012/pdf/Conference, accessed in March 2013, p.17 (2012).

Author contributions

T.M., Y.O. and A.O. designed the research and experiments. K.K. conducted the experiments and performed the data analyses. T.N. and Y.K. set up the experiments, including the high-speed camera. All authors participated in discussions, and contributed ideas throughout the project and the manuscript writing. T.M. wrote the manuscript with assistance from Y.O. and A.O.

Additional information

Competing financial interests: The authors declare no competing financial interests.

How to cite this article: Mizota, T. *et al.* The strange flight behaviour of slowly spinning soccer balls. *Sci. Rep.* **3**, 1871; DOI:10.1038/srep01871 (2013).